Observational constraints on dark energy with a fast varying equation of state

Antonio De Felice,[1,2] Savvas Nesseris,[3] and Shinji Tsujikawa[4]

[1]*TPTP & NEP, The Institute for Fundamental Study,*
Naresuan University, Phitsanulok 65000, Thailand
[2]*Thailand Center of Excellence in Physics, Ministry of Education, Bangkok 10400, Thailand*
[3]*Departamento de Fisica Teorica and Instituto de Fisica Teorica UAM/CSIC,*
Universidad Autonoma de Madrid, Cantoblanco, E-28049 Madrid, Spain
[4]*Department of Physics, Faculty of Science, Tokyo University of Science,*
1-3, Kagurazaka, Shinjuku-ku, Tokyo 162-8601, Japan
(Dated: March 1, 2013)

We place observational constraints on models with the late-time cosmic acceleration based on a number of parametrizations allowing fast transitions for the equation of state of dark energy. In addition to the model of Linder and Huterer where the dark energy equation of state w monotonically grows or decreases in time, we propose two new parametrizations in which w has an extremum. We carry out the likelihood analysis with the three parametrizations by using the observational data of supernovae type Ia, cosmic microwave background, and baryon acoustic oscillations. Although the transient cosmic acceleration models with fast transitions can give rise to the total chi square smaller than that in the Λ-Cold-Dark-Matter (ΛCDM) model, these models are not favored over ΛCDM when one uses the Akaike information criterion which penalizes the extra degrees of freedom present in the parametrizations.

I. INTRODUCTION

The discovery of the late-time cosmic acceleration [1] opened up a new research arena for cosmologists, astrophysicists, and particle physicists. From the viewpoint of particle physics the cosmological constant naturally appears as a vacuum energy of quantum fields, but its energy scale is usually very different from the observed dark energy scale [2]. As an alternative to the cosmological constant, dynamical dark energy models–such as quintessence [3], k-essence [4], $f(R)$ gravity [5], $f(R, \mathcal{G})$ gravity [6], DGP braneworld [7], and Galileon [8]–have been proposed. These models give rise to a time-varying equation of state $w(a)$ of dark energy, where a is the scale factor in the Friedmann-Lemaître-Robertson-Walker (FLRW) cosmological background [9].

At the background level it is possible to discriminate between a host of dark energy models by confronting $w(a)$ with the observations of Supernova type Ia (SN Ia), Cosmic Microwave Background (CMB), and Baryon Acoustic Oscillations (BAO). For this purpose several different parametrizations of $w(a)$ have been proposed–which are mostly based on two parameters w_0 and w_1 [10–15] (see Refs. [16, 17] for the parametrizations of the Hubble parameter H or the luminosity distance D_L instead of w). A well known example is the so-called Chevalier-Polarski-Linder (CPL) parametrization $w(a) = w_0 + w_1(1 - a)$ [11, 13], where w_0 is the value of w today ($a = 1$). The 2-parameter parametrizations have been widely used for constraining the property of dark energy [18–20].

With two parameters one usually fixes w_0 and the value of w in the asymptotic past ($= w_p$). In this case it is generally difficult to accommodate the time a_t and the width τ of the transition in two asymptotic regimes. Bassett *et al.* [21] first proposed a 4-parameter parametrization involving a_t and τ. Corasaniti and Copeland [22] further

developed this issue and proposed a *kink* parametrization given by $w(a) = w_0 + (w_p - w_0)[(1 + e^{a_t/\tau})(1 - e^{(1-a)/\tau})][(1 + e^{(a_t-a)/\tau})(1 - e^{1/\tau})]^{-1}$. This allows for quintessence models with tracker solutions having a rapid transition [23, 24], which is difficult to be addressed by the 2-parameter parametrization.

Bassett *et al.* [25] carried out the likelihood analysis with the kink parametrization by using the Gold SN Ia data [26] in 2004. They found that the best-fit corresponds to the case in which w is nearly constant ($w \sim w_p = -0.41$) for the redshift z larger than 0.1 and rapidly decreases toward $w_0 \sim -2.85$ for $z < 0.1$. This evolution of w is outside the limits of the two-parameter parametrizations, which implies that two parameters are not generally sufficient to implement such a rapid transition[1]. Corasaniti *et al.* [33] also showed that the rapidly varying equation of state is consistent with the CMB and large-scale structure data accumulated by 2004.

For the kink parametrization the Hubble parameter H cannot be derived analytically in terms of a function of a. Instead Linder and Huterer (LH) [34] proposed the 4-parameter parametrization $w(a) = w_f + (w_p - w_f)[1 + (a/a_t)^{1/\tau}]^{-1}$, which also allows a rapid transition (where w_f is the value of w in the asymptotic future). In this case there exists an explicit integrated form of $H(a)$ with respect to a, so it is technically convenient. Moreover this parametrization can accommodate tracker scaling solutions ($w_p = 0$) with the rapid decrease of w [22, 23] and thawing quintessence models ($w_p = -1$) with the fast

---

[1] In some of quintessence and k-essence models such as thawing and tracker models, it is possible to derive the analytic forms of $w(a)$ approximately [28]-[32]. Apart from the tracker models with the inverse power-law potential [32], the field equation of state usually contains more than 3 free parameters [29–31].

growth of w [35, 36].

For both the kink and the LH parametrizations the dark energy equation of state either increases or decreases monotonically. Meanwhile there are some models in which w has a minimum–such as quintessence [23], $f(R)$ gravity [37], and coupled dark energy [38] models. In order to implement models in which w has an extremum, we propose two new parametrizations given in Eqs. (7) and (12) below. These are based on four parameters a_t, τ, w_p, and w_0, which allow fast transitions of w. Moreover, in both cases, there exists analytic expression of the Hubble parameter[2].

In this paper we shall place constraints on the model parameters of the LH parametrization (5) as well as those of the parametrizations (7) and (12) by using the recent observational data of SN Ia, CMB, and BAO. In each model the five parameters a_t, τ, w_p, w_0 (or w_f), and $\Omega_m^{(0)}$ (today's density parameter of non-relativistic matter) are varied in the likelihood analysis. We also carry out the 4-parameter space analysis by fixing w_0 with a number of different values between -1 and 0. In order to accommodate the thawing-type models with fast transitions, we shall further set $w_p = -1$ and study the viability of the models (7) and (12) (including transient acceleration models) in the 3-parameter space. Note that the observational constraints on kink-like parametrizations different from those mentioned above (like those based on the deceleration parameter q) have been studied by a number of authors [40–44].

This paper is organized as follows. In Sec. II we present the three parametrizations of $w(a)$ as well as the corresponding Hubble parameter $H(a)$. In Sec. III we show the method of our likelihood analysis to confront the models with observations. In Secs. IV, V, VI we place observational constraints on the model parameters of the parametrizations (5), (7), and (12), respectively. Sec. VII is devoted to conclusions.

II. PARAMETRIZATIONS OF DARK ENERGY

We consider the flat FLRW background described by the line element $ds^2 = -dt^2 + a^2(t)d\boldsymbol{x}^2$, where t is cosmic time. We take into account dark energy with the time-varying equation of state $w(a)$ and non-relativistic matter with the density parameter $\Omega_m^{(0)}$ today. We assume that the dark energy density ρ_{DE} satisfies the continuity equation

$$\dot{\rho}_{\mathrm{DE}} + 3H(1+w)\rho_{\mathrm{DE}} = 0 \,, \qquad (1)$$

where a dot represents a derivative with respect to t, and $H = \dot{a}/a$ is the Hubble parameter. This equation can be

written in an integrated form

$$\rho_{\mathrm{DE}}(a) = \rho_{\mathrm{DE}}^{(0)} \exp\left[\int_a^1 \frac{3}{\tilde{a}}(1+w)\,d\tilde{a}\right] \,, \qquad (2)$$

where $\rho_{\mathrm{DE}}^{(0)}$ is the dark energy density today ($a = 1$). The energy density of non-relativistic matter is given by $\rho_m(a) = \rho_m^{(0)} a^{-3}$, where $\rho_m^{(0)}$ is its today's value.

The Friedmann equation gives

$$3H^2 = 8\pi G(\rho_m + \rho_{\mathrm{DE}}) \,, \qquad (3)$$

where G is the gravitational constant. This can be written as

$$\frac{H^2(a)}{H_0^2} = \Omega_m^{(0)} a^{-3} + (1 - \Omega_m^{(0)}) \exp\left[\int_a^1 \frac{3}{\tilde{a}}(1+w)d\tilde{a}\right] \,, \qquad (4)$$

where H_0 is the present value of H, $\Omega_m^{(0)} = 8\pi G \rho_m^{(0)}/(3H_0^2)$, and we used the fact that $8\pi G \rho_{\mathrm{DE}}^{(0)}/(3H_0^2) = 1 - \Omega_m^{(0)}$.

Next, we study the parametrization of dark energy allowing fast evolution of w. One of the examples is given by [34]

$$w(a) = w_f + \frac{w_p - w_f}{1 + (a/a_t)^{1/\tau}} \qquad \text{(Model 1)} \,, \qquad (5)$$

where a_t (> 0) is the scale factor at the transition epoch, and τ (> 0) characterizes the width of the transition. In the asymptotic past ($a \to 0$) and future ($a \to \infty$) one has $w \to w_p$ and $w \to w_f$, respectively. For the parametrization (5) the r.h.s. of Eq. (4) is integrated to give

$$\frac{H^2(a)}{H_0^2} = \Omega_m^{(0)} a^{-3} + (1 - \Omega_m^{(0)})$$
$$\times a^{-3(1+w_p)} \left(\frac{a^{1/\tau} + a_t^{1/\tau}}{1 + a_t^{1/\tau}}\right)^{3\tau(w_p - w_f)} \,, \quad (6)$$

which is convenient in confronting the model with observations.

However, the parametrization (5) does not accommodate the models in which w has an extremum. In order to address such cases, we propose the following parametrization

$$w(a) = w_p + (w_0 - w_p)\frac{a[1 - (a/a_t)^{1/\tau}]}{1 - a_t^{-1/\tau}} \qquad \text{(Model 2)} \,, \qquad (7)$$

where $a_t > 0$, $\tau > 0$, and w_p, w_0 are the values of w in the asymptotic past and today, respectively. For the parametrization (7) the Hubble parameter can be expressed as

$$\frac{H^2(a)}{H_0^2} = \Omega_m^{(0)} a^{-3} + (1 - \Omega_m^{(0)}) a^{-3(1+w_p)} \exp\left[f(a)\right] \,, \quad (8)$$

---

where

$$f(a) = 3(w_0 - w_p)$$
$$\times \; \frac{1 + (1 - a_t^{-1/\tau})\tau + a\{[(a/a_t)^{1/\tau} - 1]\tau - 1\}}{(1 - a_t^{-1/\tau})(1 + \tau)}. \quad (9)$$

The equation of state (7) has an extremum at

$$a_* = \left(\frac{\tau}{\tau + 1}\right)^\tau a_t, \quad (10)$$

with the value

$$w(a_*) = w_p + \frac{(w_0 - w_p)\tau^\tau(\tau + 1)^{-\tau - 1}a_t}{1 - a_t^{-1/\tau}}. \quad (11)$$

If $0 < a_t < 1$ and $w_p < w_0$, or, $a_t > 1$ and $w_p > w_0$, then w has a minimum at $a = a_*$. On the other hand, if $0 < a_t < 1$ and $w_p > w_0$, or, $a_t > 1$ and $w_p < w_0$, w has a maximum at $a = a_*$.

For the models characterized by $w_p > w_0$ with a minimum of w at $0 < a_* < 1$ (such as quintessence models in Ref. [23]), the transition redshift needs to satisfy the condition $a_t > 1$. From Eq. (10) it follows that $a_t/e < a_* < a_t$ and hence $a_* > 1/e$. This means that, for $w_p > w_0$, the parametrization (7) does not accommodate the case in which w has a minimum at low redshifts. In order to improve this shortcoming, we shall also consider the following parametrization

$$w(a) = w_p + (w_0 - w_p)\frac{a^{1/\tau}[1 - (a/a_t)^{1/\tau}]}{1 - a_t^{-1/\tau}} \quad \text{(Model 3)}, \quad (12)$$

where $a_t > 0$ and $\tau > 0$. Then w has an extremum at

$$a_* = \frac{a_t}{2^\tau}, \quad (13)$$

with the value

$$w(a_*) = w_p + \frac{1}{4}\frac{(w_0 - w_p)a_t^{1/\tau}}{1 - a_t^{-1/\tau}}. \quad (14)$$

The equation of state has a minimum either for $0 < a_t < 1$ and $w_p < w_0$, or, for $a_t > 1$ and $w_p > w_0$. Since $a_* \to 0$ for $\tau \gg 1$, we can cover the case of small a_* even for $a_t > 1$ and $w_p > w_0$.

The Hubble parameter corresponding to the parametrization (12) is given by Eq. (8), where the function $f(a)$ is

$$f(a) = 3(w_0 - w_p)\tau$$
$$\times \; \frac{2 - a_t^{-1/\tau} + a^{1/\tau}[(a/a_t)^{1/\tau} - 2]}{2(1 - a_t^{-1/\tau})}. \quad (15)$$

In the regime $0 < a < 1$ the parametrizations (5), (7), and (12) can recover the CPL parametrization $w(a) = w_0 + w_1(1 - a)$ in the limit that $a_t \gg 1$ (with $\tau = 1$ for Model 1 and Model 3).

III. DATA ANALYSIS

In this section we explain the method employed to constrain Models 1, 2, and 3 observationally. In our analysis we use the three datasets: 1) the SN Ia (Constitution [45]); 2) the CMB shift parameters (WMAP7) [19]; 3) the BAO (SDSS7) [46]. The flat Universe is assumed throughout the analysis.

In SN Ia observations the apparent magnitude $m(z)$ at peak brightness is related with the luminosity distance $d_L(z) = (1 + z)\int_0^z H^{-1}(\tilde{z})d\tilde{z}$ through $m(z) = M + 5\log_{10}(d_L(z)/10\,\text{pc})$, where $z = 1/a - 1$ is the redshift and M is the absolute magnitude [1]. We define the distance modulus

$$\mu(z) \equiv m(z) - M = 5\log_{10}[H_0 d_L(z)] + \mu_0, \quad (16)$$

where $\mu_0 = 42.38 - 5\log_{10} h$ with $h = H_0/[100\,\text{km}\,\text{sec}^{-1}\,\text{Mpc}^{-1}]$. The chi square associated with SN Ia observations is given by

$$\chi^2_{\text{SN Ia}} = \sum_{i=1}^N \frac{\mu_{\text{obs}}(z_i) - \mu(z_i)}{\sigma^2_{\mu,i}}, \quad (17)$$

where N is the number of the SN Ia dataset, $\mu_{\text{obs}}(z_i)$ are the observed values of the distance modulus, and $\sigma_{\mu,i}$ are the errors on the data. We employ the Constitution dataset with the total of 397 SN Ia in order to find the minimum of (17) and the corresponding best-fit parameters.

The position of the CMB acoustic peaks can be quantified by the following two parameters [47]

$$\mathcal{R} = \sqrt{\Omega_m^{(0)}} \int_0^{z_*} \frac{dz}{H(z)/H_0}, \qquad l_a = \frac{\pi d_a^{(c)}(z_*)}{r_s(z_*)}, \quad (18)$$

where z_* is the redshift at the decoupling epoch, $d_a^{(c)}(z_*) = \mathcal{R}/[H_0\sqrt{\Omega_m^{(0)}}]$ is the comoving angular diameter distance to the last scattering surface, and $r_s(z_*)$ is the sound horizon defined by

$$r_s(z_*) = \int_{z_*}^\infty \frac{dz}{H(z)\sqrt{3\{1 + 3\Omega_b^{(0)}/[4\Omega_\gamma^{(0)}(1 + z)]\}}}. \quad (19)$$

Here $\Omega_b^{(0)}$ and $\Omega_\gamma^{(0)}$ are the density parameters of baryons and photons, respectively. For the redshift z_* there exists the following fitting formula [48]

$$z_* = 1048\,[1 + 0.00124(\Omega_b^{(0)}h^2)^{-0.738}]\,[1 + g_1\,(\Omega_m^{(0)}h^2)^{g_2}], \quad (20)$$

where $g_1 = 0.0783\,(\Omega_b^{(0)}h^2)^{-0.238}/[1 + 39.5\,(\Omega_b^{(0)}h^2)^{0.763}]$ and $g_2 = 0.560/[1 + 21.1\,(\Omega_b^{(0)}h^2)^{1.81}]$. The chi square for the WMAP7 measurement is

$$\chi^2_{\text{CMB}} = \boldsymbol{X}^T_{\text{CMB}}\boldsymbol{C}^{-1}_{\text{CMB}}\boldsymbol{X}_{\text{CMB}}, \quad (21)$$

where $\boldsymbol{X}_{\mathrm{CMB}}^T = (l_a - 302.09, \mathcal{R} - 1.725, z_* - 1091.3)$, and the inverse covariance matrix is given by [19]

$$C_{\mathrm{CMB}}^{-1} = \begin{pmatrix} 2.305 & 29.698 & -1.333 \\ 29.698 & 6825.27 & -113.18 \\ -1.333 & -113.18 & 3.414 \end{pmatrix}. \quad (22)$$

The BAO observations constrain the ratio $r_{\mathrm{BAO}}(z) \equiv r_s(z_d)/D_V(z)$, where $r_s(z_d)$ is the sound horizon at which the baryons are released from the Compton drag of photons (denoted as the redshift z_d). $D_V(z)$ is the effective BAO distance defined by $D_V(z) \equiv [d_a^{(c)}(z)^2 z/H(z)]^{1/3}$ [49], where $d_a^{(c)}(z) = \int_0^z H^{-1}(\tilde{z})d\tilde{z}$. For the redshift z_d there is the following fitting formula [50]

$$z_d = \frac{1291\,(\Omega_m^{(0)}h^2)^{0.251}}{1 + 0.659\,(\Omega_m^{(0)}h^2)^{0.828}} [1 + b_1\,(\Omega_b^{(0)}h^2)^{b_2}], \quad (23)$$

where $b_1 = 0.313\,(\Omega_m^{(0)}h^2)^{-0.419}[1 + 0.607\,(\Omega_m^{(0)}h^2)^{0.674}]$ and $b_2 = 0.238(\Omega_m^{(0)}h^2)^{0.223}$. The chi square associated with the BAO measurement is given by

$$\chi_{\mathrm{BAO1}}^2 = \boldsymbol{X}_{\mathrm{BAO}}^T C_{\mathrm{BAO}}^{-1} \boldsymbol{X}_{\mathrm{BAO}}, \quad (24)$$

where $\boldsymbol{X}_{\mathrm{BAO}}^T = (r_{\mathrm{BAO}}(0.2) - 0.1905, r_{\mathrm{BAO}}(0.35) - 0.1097)$, and the inverse covariance matrix is [46]

$$C_{\mathrm{BAO}}^{-1} = \begin{pmatrix} 30124 & -17227 \\ -17227 & 86977 \end{pmatrix}. \quad (25)$$

We also use the BAO data from the WiggleZ and 6dFGS surveys. These data are given in terms of $A(z)$, where its theoretical value is

$$A_{\mathrm{th}}(z) \equiv \frac{D_V(z)\sqrt{\Omega_m^{(0)}H_0^2}}{z}, \quad (26)$$

and the data are $A_{\mathrm{WiggleZ}}(z = 0.6) = 0.452 \pm 0.018$ [51] and $A_{\mathrm{6dFGS}}(z = 0.106) = 0.526 \pm 0.028$ [52]. The chi-square is given by

$$\chi_{\mathrm{BAO2}}^2 = \sum_{i=1}^2 \left(\frac{A(z_i) - A_{\mathrm{th}}(z_i)}{\sigma_i} \right)^2. \quad (27)$$

Therefore, the total chi-square from the three datasets is

$$\chi^2 = \chi_{\mathrm{SNIa}}^2 + \chi_{\mathrm{CMB}}^2 + \chi_{\mathrm{BAO1}}^2 + \chi_{\mathrm{BAO2}}^2. \quad (28)$$

The best-fit corresponds to the model parameters for which the χ^2 is minimized.

IV. OBSERVATIONAL CONSTRAINTS ON MODEL 1

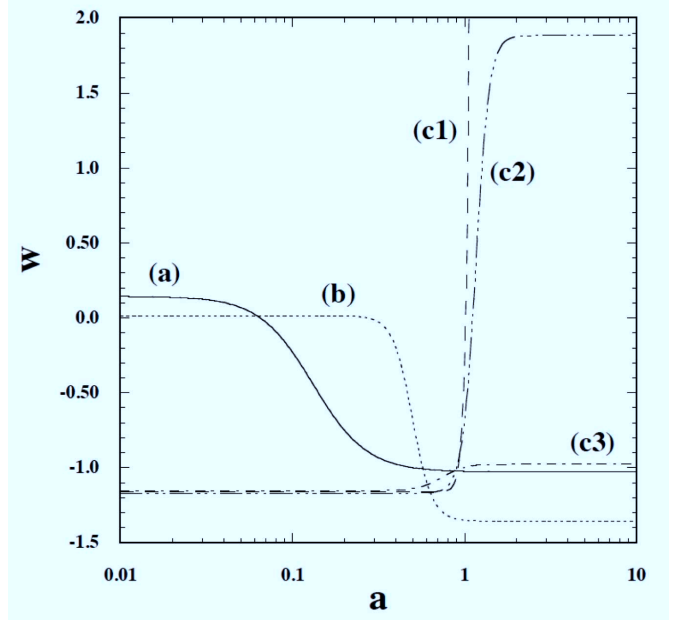We place observational constraints on Model 1 according to the method explained in Sec. III.

Figure 1: The dark energy equation of state w versus the scale factor a for Model 1 with several different model parameters. The line (a) corresponds to the best-fit case of Eq. (29) derived by varying the 5 parameters $w_p, w_f, a_t, \tau, \Omega_m^{(0)}$ in the likelihood analysis. The line (b) shows the best-fit derived with the priors $w_p \geq 0$ and $a_t \geq 0.5$. The lines (c1), (c2), (c3) represent the best-fits where the 4 parameters $w_p, a_t, \tau, \Omega_m^{(0)}$ are varied with the present value of the equation of state fixed at $w_0 = -1/3, -0.7, -1$, respectively.

We first vary the 5 parameters w_p, w_f, a_t, τ, and $\Omega_m^{(0)}$ in the likelihood analysis. The priors on each parameter are set to be $-10 \leq w_p \leq 10$, $-10 \leq w_f \leq 10$, $a_t > 0$, $\tau > 0$, and $0.15 < \Omega_m^{(0)} < 0.4$. We find that the best-fit parameters are

$$w_p = 0.141866, \quad w_f = -1.02862, \quad a_t = 0.132023,$$
$$\tau = 0.360069, \quad \Omega_m^{(0)} = 0.290346, \quad (29)$$

with $\chi^2 = 467.77$. In Fig. 1 we plot the evolution of w for the best-fit case [line (a)]. Initially there is a period where w stays nearly constant ($w \simeq 0.14$), which is followed by the decrease of w around the redshift z larger than 10. The dark energy equation of state crosses the cosmological constant boundary ($w = -1$) around $z = 1$ and it approaches the asymptotic value $w_f = -1.028$.

If w starts to evolve from the value larger than 0 in the deep matter era, it is required that the transition to the regime $w \approx -1$ occurs in the early cosmological epoch (for z larger than 1). In fact, if we carry out the likelihood analysis with the priors $w_p \geq 0$ and $a_t \geq 0.5$, the best-fit model parameters are found to be

$$w_p = 0.0120045, \quad w_f = -1.35856, \quad a_t = 0.5,$$
$$\tau = 0.130893, \quad \Omega_m^{(0)} = 0.300473, \quad (30)$$

w_0	w_p	a_t	τ	$\Omega_m^{(0)}$	χ^2
0	-1.04279	1.20514	0.00277414	0.276338	470.825
$-1/3$	-1.16253	1.31208	0.0502325	0.280804	471.530
-0.5	-1.17027	1.30959	0.0659688	0.281219	470.996
-0.6	-1.17165	1.26349	0.0779737	0.281295	470.707
-0.7	-1.17077	1.16698	0.0907055	0.281248	470.456
-0.8	-1.16655	1.18425	0.116396	0.280961	470.276
-1	-1.15384	0.742678	0.15533	0.279799	470.387

Table I: The best-fit model parameters (4 parameters in total) and χ^2 for Model 1 with several given values of w_0.

with $\chi^2 = 505.983$. In this case, the bound on a_t is saturated at $a_t = 0.5$ and the best-fit χ^2 is much larger than that corresponding to Eq. (29). Since $\tau \ll 1$, the transition from the regime $w \geq 0$ to the regime $w \approx -1$ occurs quite rapidly. In Fig. 1 we compare the behavior of the two best-fits in Eqs. (29) and (30).

The likelihood analysis of Bassett *et al.* [25] for the kink parametrization, with the SN Ia and CMB data accumulated by 2004, showed that the best fit corresponds to the fast transition in low redshifts ($z < 0.1$). However, inclusion of the BAO data as well as the more updated SN Ia and CMB data, seems to point towards a much earlier transition from the regime $w \sim 0$ to the regime close to $w = -1$.

In order to study the possibility of the late-time transition further, we also study the case in which the value of w today ($= w_0$) is fixed. Since $w_f = a_t^{1/\tau}[w_0(1+a_t^{-1/\tau}) - w_p]$, the parametrization (5) can be expressed as

$$w(a) = \frac{w_p + a^{1/\tau}[w_0(1 + a_t^{-1/\tau}) - w_p]}{1 + (a/a_t)^{1/\tau}}. \qquad (31)$$

For several given values of w_0 we vary the 4 parameters w_p, a_t, τ, and $\Omega_m^{(0)}$ with the priors $-10 \leq w_p \leq 10$, $a_t > 0$, $\tau > 0$, and $0.15 < \Omega_m^{(0)} < 0.4$. In Table I the best-fit model parameters and the corresponding χ^2 are shown for $w_0 = 0, -1/3, -0.5, -0.6, -0.7, -0.8, -1$. In Fig. 1 we also plot w versus a for several different best-fit cases ($w_0 = -1/3, -0.7, -1$).

For the values of w_0 between -1 and 0, the initial evolution of w for each case shown in Table I exhibits a common property. The dark energy equation of state is nearly constant with w less than -1 during the deep matter era, which is followed by the growth of w in the low-redshift regime ($z \lesssim 1$). The parameter τ tends to be smaller for larger w_0, so that the transition becomes sharper. This property can be confirmed by comparing the three best-fit cases (c1)-(c3) in Fig. 1.

In Table I we find that χ^2 is more or less similar for different choices of w_0 between -1 and 0. The best-fit ΛCDM model corresponds to $\Omega_m^{(0)} = 0.269431$ with $\chi^2 = 471.89$, whose χ^2 is larger than those given in Table I. This implies that the transient cosmic acceleration models with rapid transitions of w are not excluded by the current observational data.

We need to caution, however, that the parametrization (31) with given w_0 has 4 free parameters to fit the models with the data, while the ΛCDM model has only one free parameter ($\Omega_m^{(0)}$). In order to compare the models with different number of free parameters, we employ the Akaike Information Criterion (AIC) [53]. The AIC is defined as

$$\text{AIC} = \chi^2_{\min} + 2\mathcal{P}, \qquad (32)$$

where $\chi^2_{\min}$ is the minimum value of χ^2, and $\mathcal{P}$ is the number of free parameters for each model. For smaller AIC the model is more favored. If the difference of AIC between two models is in the range $0 < \Delta(\text{AIC}) < 2$, the models are considered to be equivalent. On the other hand, if $\Delta(\text{AIC}) > 2$, one model is favored over another one.

The flat ΛCDM model corresponds to AIC = 473.89, whereas the transient acceleration models in Table I give rise to larger values of AIC (e.g., AIC = 478.825 for $w_0 = 0$). The best-fit case (29) with 5 parameters corresponds to AIC = 477.77. According to the AIC, Model 1 with 5 or 4 free parameters is not favored over the ΛCDM model.

V. OBSERVATIONAL CONSTRAINTS ON MODEL 2

Let us proceed to observational constraints on Model 2. We first vary the 5 parameters w_p, w_0, a_t, τ, and $\Omega_m^{(0)}$ in the likelihood analysis. We set the priors on each parameter, as $-10 \leq w_p \leq 10$, $-10 \leq w_0 \leq 10$, $a_t > 0$, $\tau > 0$, and $0.15 < \Omega_m^{(0)} < 0.4$. The best-fit parameters are found to be

$$w_p = -1.10237, \quad w_0 = -0.906508, \quad a_t = 0.739325,$$
$$\tau = 0.505998, \quad \Omega_m^{(0)} = 0.280583, \qquad (33)$$

with $\chi^2 = 470.241$. In this case χ^2 is smaller than that in the ΛCDM model, but it is larger than that in the best-fit case (29) of Model 1.

In Fig. 2 the evolution of w for the parameters (33) is plotted as the solid line (a). As we showed in Sec. II, w has a minimum at a_* given in Eq. (10) either for (i) $0 < a_t < 1$, $w_p < w_0$, or (ii) $a_t > 1$, $w_p > w_0$. The best-fit model parameters (33) correspond to the case (i) with $a_* = 0.43$. The equation of state starts from a phantom value $w_p = -1.10237$, which is followed by mild decrease of w. For $a > a_*$ it starts to increase and reaches the present value $w_0 = -0.906508$.

The above behavior of w is different from that for the best-fit Model 1 with 5 parameters varied. As we see in Fig. 1 the best-fit parameters in Model 1 satisfy the condition $w_p > w_0$, but in this case Model 2 gives rise to a minimum only for $a_t > 1$. Since a_* is limited in the range $a_t/e < a_* < a_t$ and also τ is required to be large ($\tau \gg 1$) to have small a_*, it becomes more difficult to fit
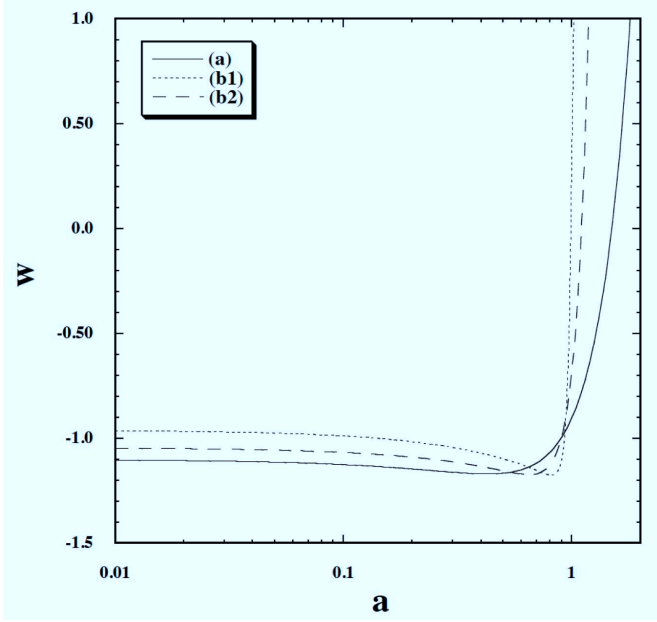
w_0	w_p	a_t	τ	$\Omega_m^{(0)}$	χ^2
0	−1	0.940663	0.0319267	0.277496	472.984
−1/3	−1	0.916762	0.0689972	0.280277	471.702
−0.5	−1	0.909223	0.0938171	0.280760	471.074
−0.7	−1	0.901454	0.1517700	0.280844	470.476
−0.9	−1	0.897160	0.7207540	0.280662	470.245

Table III: The best-fit model parameters (3 parameters in total) and χ^2 for Model 2 with $w_p = -1$ and several given values of w_0.

Figure 2: The dark energy equation of state w versus a for Model 2. The line (a) corresponds to the 5-parameter best-fit case given in Eq. (33). The lines (b1) and (b2) show the best-fits where the 4 parameters $w_p, a_t, \tau, \Omega_m^{(0)}$ are varied with $w_0 = 0, -0.7$, respectively.

w_0	w_p	a_t	τ	$\Omega_m^{(0)}$	χ^2
0	−0.96206	0.93842	0.04200	0.27847	473.130
−1/3	−1.05556	0.90118	0.06302	0.28045	471.638
−0.5	−1.14904	0.80038	0.07330	0.28111	471.001
−0.7	−1.04574	0.87618	0.14101	0.28095	470.468
−0.9	−0.97634	0.92387	0.77675	0.28064	470.246

Table II: The best-fit model parameters (4 parameters in total) and χ^2 for Model 2 with several given values of w_0.
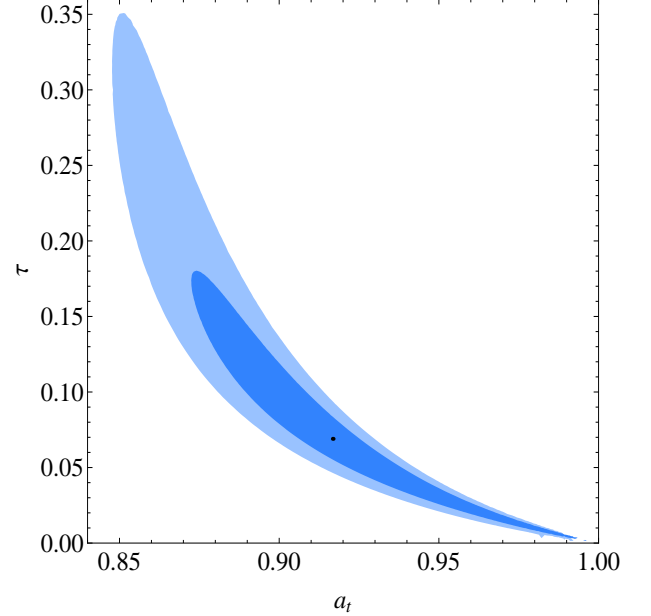

Figure 3: The 1σ (inside) and 2σ (outside) likelihood contours in the (a_t, τ) plane derived by varying the 2 parameters a_t and τ with $w_p = -1$, $w_0 = -1/3$, and $\Omega_m^{(0)} = 0.280277$ for Model 2. The black point corresponds to the best-fit case.

w with the observational data for $a_t > 1$ and $w_p > w_0$. If $w_p > w_0$ and $0 < a_t < 1$, w has a maximum at $a = a_*$. However, such cases are also difficult to be compatible with the observational data.

By choosing several different values of w_0 (= $0, -1/3, -0.5, -0.7, -0.9$), we also vary the 4 parameters $w_p, a_t, \tau, \Omega_m^{(0)}$ in the likelihood analysis. The priors are set to be $-10 \le w_p \le 10$, $a_t > 0$, $\tau > 0$, and $0.15 < \Omega_m^{(0)} < 0.4$. In Table. II we show the best-fit parameters and χ^2 for each w_0. In all cases we find that $0 < a_t < 1$ and $w_p < w_0$, so that w has a minimum at $0 < a_* < 1$.

In Fig. 2 we show the variation of w for the best-fit cases with $w_0 = 0$ and $w_0 = -0.7$ as the lines (b1) and (b2), respectively. The growth of w in the regime $a > a_*$ is sharper for larger values of w_0. This reflects the fact that, in Table II, τ gets smaller for w_0 increased. We also note that the models with larger w_0 tend to be disfavored

because of the increase of χ^2 seen in Table II.

In addition to w_0, we also fix w_p to be -1 and vary the 3 parameters $a_t, \tau, \Omega_m^{(0)}$. In Table III we present the best-fit model parameters for several different choices of w_0 (> -1). In all cases the transition scale factor is in the range $0 < a_t < 1$, so that w has a minimum for $0 < a_* < 1$. In fact, the evolution of w starting from -1 and having a minimum by today is present for dark energy models based on $f(R)$ theories [37] (although w does not continuously grow for $a > 1$). Table III shows that, for larger w_0, τ tends to be smaller, whereas χ^2 gets larger.

In Fig. 3 we illustrate the 1σ and 2σ observational contours in the (a_t, τ) plane for $w_p = -1$, $w_0 = -1/3$, and $\Omega_m^{(0)} = 0.280277$. This is the marginal case in which the Universe enters the phase of cosmic deceleration today. The redshift and the width of the transition are constrained to be $0.87 < a_t < 0.99$ and $0 < \tau < 0.18$ (68% CL). Unless the rapid transition occurs at the redshift

close to today, the model is not compatible with the observational data. For larger τ the values of w at $a = a_*$ start to deviate from -1, so that those cases are more difficult to satisfy observational constraints.

As mentioned in Sec. IV, the AIC for the flat ΛCDM model is AIC $= 473.89$. For the 5-parameter best-fit case in Eq. (33) and for the 4-parameter and 3-parameter best-fit cases given in Tables II and III, the AIC in each model is larger than that in the ΛCDM model with the difference more than 2. Hence the AIC criterion shows that the ΛCDM is generally favored over Model 2.

VI. OBSERVATIONAL CONSTRAINTS ON MODEL 3

Finally we proceed to observational constraints on Model 3. When the 5 parameters $w_p, w_0, a_t, \tau, \Omega_m^{(0)}$ are varied in the likelihood analysis, we set the same priors as those given in Model 2. The best-fit parameters are found to be

$$w_p = -1.10733, \quad w_0 = -0.897454, \quad a_t = 0.737871,$$
$$\tau = 0.652107, \quad \Omega_m^{(0)} = 0.28053, \tag{34}$$

with $\chi^2 = 470.235$.

As we see in Fig. 4, the evolution of w corresponding to Eq. (34) is similar to that for the best-fit parameters (33) of Model 2. Since $0 < a_t < 1$ and $w_p < w_0$ for the model parameters (34), w has a minimum at $a_* = 0.47$. The difference between Models 2 and 3 is that even for $a_t > 1$ and $w_p > w_0$ the equation of state for Model 3 can take minima with smaller values of a_* given in Eq. (13). However we find that the models with $a_t > 1$ and $\tau \gg 1$ are disfavored because $w(a_*)$ deviates from -1.

For the 4-parameter parametrization with a number of different values of w_0 ($= 0, -1/3, -0.5, -0.7, -0.9$) we also vary the parameters $w_p, a_t, \tau, \Omega_m^{(0)}$ with the same priors used for Model 2. In Table IV we summarize the best-fit parameters as well as the χ^2 for each w_0. For $w_0 = -1/3, -0.5, -0.7$ one has $0 < a_t < 1$ and $w_p < w_0$, in which cases w has minima at $0 < a_* < 1$. If $w_0 > -0.5$, the growth of w in the regime $a > a_*$ is very rapid (see the line (b1) in Fig. 4).

For the best-fit parameters corresponding to $w_0 = 0, -0.9$ one has $a_t > 1$ and $w_p < w_0$. In those cases w has maxima at a_* larger than 1 and hence w is a growing function for $a < 1$. Since τ is extremely small for $w_0 = 0$, the transition of w occurs almost like a step function. However such an instant transition cannot be regarded as a realistic model of dark energy. For $w_0 = -0.9$, w has a maximum ($w(a_*) = 5.5$) at $a_* = 2.4$. In this case the evolution of w is not very different from that for the best-fit case (34), apart from the fact that for $w_0 = -0.9$ the equation of state is a growing function in the regime $a < 1$.

We also vary the 3 parameters $a_t, \tau, \Omega_m^{(0)}$ by fixing w_p to be -1 for several different choices of w_0 (> -1). In Table
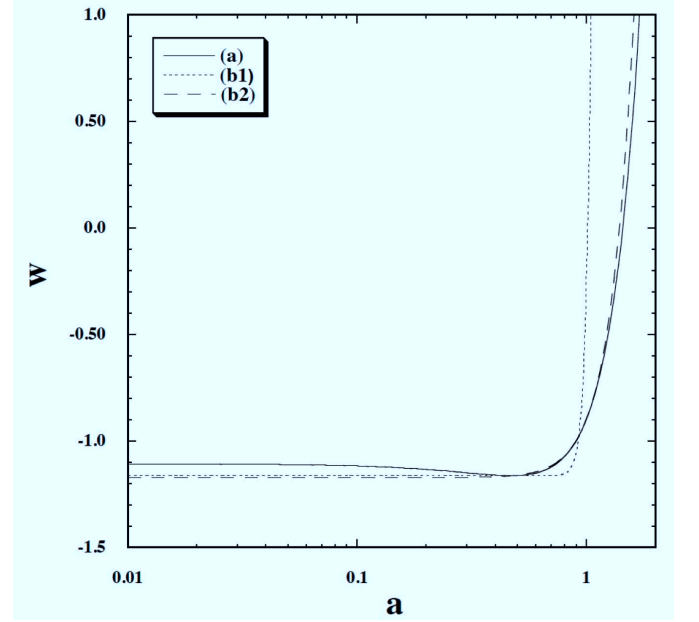

Figure 4: The dark energy equation of state w versus a for Model 3. The line (a) represents the 5-parameter best-fit case given in Eq. (34), whereas the lines (b1) and (b2) correspond to the best-fits derived by varying the 4 parameters $w_p, a_t, \tau, \Omega_m^{(0)}$ with $w_0 = -1/3, -0.9$, respectively.

w_0	w_p	a_t	τ	$\Omega_m^{(0)}$	χ^2
0	-1.04278	3.86853	5.86338×10^{-13}	0.27634	470.825
$-1/3$	-1.16195	0.68613	0.10267	0.28079	471.533
-0.5	-1.16009	0.78777	0.15968	0.28113	471.001
-0.7	-1.06189	0.86545	0.35609	0.28086	470.468
-0.9	-1.17212	2.75038	0.22092	0.28049	470.234

Table IV: The best-fit model parameters (4 parameters in total) and χ^2 for Model 3 with several given values of w_0.

w_0	w_p	a_t	τ	$\Omega_m^{(0)}$	χ^2
0	-1	0.918824	0.185756	0.277967	474.087
$-1/3$	-1	0.909047	0.249165	0.279820	472.013
-0.5	-1	0.904406	0.296622	0.280332	471.194
-0.7	-1	0.899265	0.398049	0.280590	470.495
-0.9	-1	0.901692	0.788501	0.280323	470.242

Table V: The best-fit model parameters (3 parameters in total) and χ^2 for Model 3 with $w_p = -1$ and several given values of w_0.

V we show the best-fit values as well as χ^2 for each w_0. In most cases the transition redshifts are around $a_t = 0.9$. As we increase w_0 the parameter τ gets smaller, so that the transition occurs more rapidly. For larger w_0, χ^2 tends to be larger.

In Fig. 5 we plot observational bounds in the (a_t, τ) plane for $w_p = -1$, $w_0 = -1/3$, and $\Omega_m^{(0)} = 0.279820$.
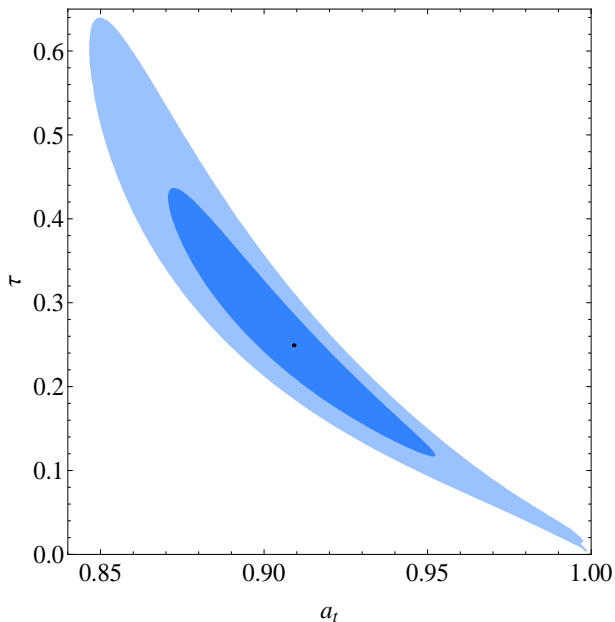
Figure 5: The 1σ (inside) and 2σ (outside) likelihood contours in the (a_t, τ) plane derived by varying the 2 parameters a_t and τ with $w_p = -1$, $w_0 = -1/3$, and $\Omega_m^{(0)} = 0.279820$ for Model 3. The black point corresponds to the best-fit case.

Comparing it to Fig. 3, we find that the larger values of τ can be allowed in Model 3. This reflects the fact that in Model 3 the values of $w(a_*)$ do not deviate from -1 significantly for $\tau \lesssim 0.5$. The two parameters are constrained to be $0.87 < a_t < 0.95$ and $0.12 < \tau < 0.44$ (68% CL).

For all the best-fit cases discussed above, the AIC is larger than that in the flat ΛCDM model. Hence Model 3 is not favored over the ΛCDM model according to the AIC.

VII. CONCLUSIONS

In this paper we placed observational constraints on the three models allowing fast transitions of w, by using the data of SN Ia, CMB shift parameters, and BAO. Unlike the 2-parameter parametrization such as $w(a) = w_0 + w_1(1 - a)$, the parametrizations (5), (7), and (12) have two more parameters a_t and τ by which the time and the width of the transition can be accommodated. In Model 1 the dark energy equation of state monotonically increases or decreases in time, whereas in Models 2 and 3 w has either a minimum or a maximum depending on the values of w_p, w_0, and a_t. For all these models the Hubble parameter H is analytically known in terms of functions of a.

When the 5 parameters $w_p, w_f, a_t, \tau, \Omega_m^{(0)}$ are varied in Model 1, the best-fit parameters are given by Eq. (29) with $\chi^2 = 467.77$. This corresponds to the solid curve (a) in Fig. 1, in which case the equation of state enters

the regime $w \sim -1$ in the early cosmological epoch. If we put the prior on the transition redshift as $a_t > 0.5$, χ^2 becomes significantly larger than that without a prior on a_t. This means that the late-time transition ($a_t > 0.5$) from the regime $w \sim 0$ to the regime $w \sim -1$ is disfavored observationally. If we vary the 4 parameters $w_p, a_t, \tau, \Omega_m^{(0)}$ with several different values of w_0 between -1 and 0, the parameter τ tends to be smaller for increasing w_0. Although the χ^2 in Model 1 with 5 or 4 parameters can be smaller than that in the ΛCDM model, the AIC shows that Model 1 is not favored over the ΛCDM model.

The best-fit parameters for Model 2 corresponds to the case in which w starts from a phantom value $w_p = -1.10$, takes a minimum -1.17 at $a_* = 0.43$, and grows to the value $w_0 = -0.91$ by today. This is different from the evolution of w for the best-fit parameters of Model 1. This difference mainly comes from the fact that, in the cases $w_p > w_0$ for Model 2, w has a minimum at a_* given by Eq. (10) only for $a_t > 1$. While Model 2 can accommodate the late-time transition having a minimum of w, it is difficult to address the early sharp transition with $w_p > w_0$. The 4-parameter likelihood analysis for a number of fixed w_0 (between -1 and 0) leads to similar best-fit evolution of w to that for the 5-parameter best-fit case, with a faster transition for larger w_0.

In Model 3 the equation of state has an extremum at $a_* = a_t/2^\tau$, which can be smaller that that for Model 2. If $w_p > w_0$, however, the early transition of w with a minimum requires the condition $\tau \gg 1$. This value of τ is too large to accommodate the early transition compatible with observations, because the minimum value of w tends to deviate from -1. The 5-parameter likelihood analysis shows that the best-fit case in Model 3 is similar to that in Model 2. The likelihood results for 4 parameters (w_0 fixed) and for 3 parameters (w_0 and w_p fixed) also give rise to the similar results to those found in Model 2.

In Models 2 and 3 the AIC is always larger than that in the ΛCDM model with the difference more than 2. Hence the models with the late-time fast transition to the non-accelerating Universe are disfavored compared to the ΛCDM model. The joint data analysis based on SN Ia, CMB, and BAO prefers the models in which w do not deviate significantly from -1 in the low-redshift regime.

Although the minimum value of χ^2 in Model 1 with 5 parameters is smaller than those in Models 2 and 3, the minima in Models 2 and 3 are still inside the 1σ region corresponding to Model 1. Therefore we cannot prefer/exclude any parametrization with respect to any other one.

Recently it was shown that, in the framework of the CPL parametrization, the observational constraints on dark energy are sensitive to the presence of the cosmic curvature $\Omega_K^{(0)}$ [54]. They found that the CPL parametrization is not sufficiently flexible to model the rapidly varying equation of state in low redshifts even for $\Omega_K^{(0)} \neq 0$ (see also Ref. [43]). It will be of interest to study how the effect of the cosmic curvature affects the

observational constraints on the models discussed in this paper. We leave this for future work.

[1] A. G. Riess *et al.* [Supernova Search Team Collaboration], Astron. J. **116**, 1009 (1998); S. Perlmutter *et al.* [Supernova Cosmology Project Collaboration], Astrophys. J. **517**, 565 (1999).

[2] S. Weinberg, Rev. Mod. Phys. **61**, 1 (1989).

[3] Y. Fujii, Phys. Rev. D **26**, 2580 (1982); L. H. Ford, Phys. Rev. D **35**, 2339 (1987); C. Wetterich, Nucl. Phys B. **302**, 668 (1988); B. Ratra, P. J. E. Peebles, Phys. Rev. **D37**, 3406 (1988); T. Chiba, N. Sugiyama and T. Nakamura, Mon. Not. Roy. Astron. Soc. **289**, L5 (1997); P. G. Ferreira and M. Joyce, Phys. Rev. Lett. **79**, 4740 (1997); R. R. Caldwell, R. Dave and P. J. Steinhardt, Phys. Rev. Lett. **80**, 1582 (1998).

[4] C. Armendariz-Picon, T. Damour and V. F. Mukhanov, Phys. Lett. **B458**, 209-218 (1999); T. Chiba, T. Okabe and M. Yamaguchi, Phys. Rev. **D62**, 023511 (2000); C. Armendariz-Picon, V. F. Mukhanov and P. J. Steinhardt, Phys. Rev. Lett. **85**, 4438-4441 (2000).

[5] S. Capozziello, Int. J. Mod. Phys. D **11**, 483 (2002); S. Capozziello, S. Carloni and A. Troisi, Recent Res. Dev. Astron. Astrophys. **1**, 625 (2003); S. M. Carroll, V. Duvvuri, M. Trodden and M. S. Turner, Phys. Rev. D **70**, 043528 (2004).

[6] S. M. Carroll, A. De Felice, V. Duvvuri, D. A. Easson, M. Trodden and M. S. Turner, Phys. Rev. D **71**, 063513 (2005); S. Nojiri and S. D. Odintsov, Phys. Lett. B **631**, 1 (2005); A. De Felice and S. Tsujikawa, Phys. Lett. B **675**, 1 (2009); A. De Felice and T. Suyama, JCAP **0906**, 034 (2009); A. De Felice and T. Tanaka, Prog. Theor. Phys. **124**, 503 (2010).

[7] G. R. Dvali, G. Gabadadze and M. Porrati, Phys. Lett. B **485**, 208 (2000).

[8] A. Nicolis, R. Rattazzi and E. Trincherini, Phys. Rev. D **79**, 064036 (2009); C. Deffayet, G. Esposito-Farese and A. Vikman, Phys. Rev. D **79**, 084003 (2009); A. De Felice and S. Tsujikawa, Phys. Rev. Lett. **105**, 111301 (2010); Phys. Rev. D **84**, 124029 (2011).

[9] V. Sahni and A. A. Starobinsky, Int. J. Mod. Phys. D **9**, 373 (2000); S. M. Carroll, Living Rev. Rel. **4**, 1 (2001); T. Padmanabhan, Phys. Rept. **380**, 235 (2003); P. J. E. Peebles and B. Ratra, Rev. Mod. Phys. **75**, 559 (2003); E. J. Copeland, M. Sami and S. Tsujikawa, Int. J. Mod. Phys. D **15**, 1753 (2006); T. P. Sotiriou and V. Faraoni, Rev. Mod. Phys. **82**, 451 (2010); A. De Felice and S. Tsujikawa, Living Rev. Rel. **13**, 3 (2010); S. Tsujikawa, Lect. Notes Phys. **800**, 99 (2010); arXiv:1004.1493 [astro-ph.CO].

[10] D. Huterer and M. S. Turner, Phys. Rev. D **64**, 123527 (2001).

[11] M. Chevallier and D. Polarski, Int. J. Mod. Phys. D **10**, 213 (2001).

[12] J. Weller and A. J. Albrecht, Phys. Rev. D **65**, 103512 (2002).

[13] E. V. Linder, Phys. Rev. Lett. **90**, 091301 (2003).

[14] H. K. Jassal, J. S. Bagla and T. Padmanabhan, Mon. Not. Roy. Astron. Soc. **356**, L11 (2005).

[15] G. Efstathiou, Mon. Not. R. Astron. Soc. **342**, 810 (2000).

[16] T. D. Saini, S. Raychaudhury, V. Sahni and A. A. Starobinsky, Phys. Rev. Lett. **85**, 1162 (2000); U. Alam, V. Sahni, T. D. Saini and A. A. Starobinsky, Mon. Not. Roy. Astron. Soc. **344**, 1057 (2003); U. Alam, V. Sahni, T. D. Saini and A. A. Starobinsky, Mon. Not. Roy. Astron. Soc. **354**, 275 (2004).

[17] V. Sahni and A. Starobinsky, Int. J. Mod. Phys. D **15**, 2105 (2006).

[18] I. Maor, R. Brustein, J. McMahon and P. J. Steinhardt, Phys. Rev. D **65**, 123003 (2002); Y. Wang and P. Mukherjee, Astrophys. J. **606**, 654 (2004); A. Upadhye, M. Ishak and P. J. Steinhardt, Phys. Rev. D **72**, 063501 (2005); Z. K. Guo, N. Ohta and Y. Z. Zhang, Phys. Rev. D **72**, 023504 (2005); Astrophys. J. **650**, 1 (2006); S. Nesseris and L. Perivolaropoulos, Phys. Rev. D **70**, 043531 (2004); R. Lazkoz, S. Nesseris and L. Perivolaropoulos, JCAP **0511**, 010 (2005); S. Nesseris and L. Perivolaropoulos, JCAP **0702**, 025 (2007); R. Crittenden, E. Majerotto and F. Piazza, Phys. Rev. Lett. **98**, 251301 (2007); K. Ichikawa and T. Takahashi, JCAP **0702**, 001 (2007); G. B. Zhao, J. Q. Xia, B. Feng and X. Zhang, Int. J. Mod. Phys. D **16**, 1229 (2007); G. B. Zhao *et al.,* Phys. Lett. B **648**, 8 (2007).

[19] E. Komatsu *et al.* [WMAP Collaboration], Astrophys. J. Suppl. **192**, 18 (2011).

[20] N. Suzuki *et al.*, Astrophys. J. **746**, 85 (2012).

[21] B. A. Bassett, M. Kunz, J. Silk and C. Ungarelli, Mon. Not. Roy. Astron. Soc. **336**, 1217 (2002).

[22] P. S. Corasaniti and E. J. Copeland, Phys. Rev. D **67**, 063521 (2003).

[23] T. Barreiro, E. J. Copeland and N. J. Nunes, Phys. Rev. D **61**, 127301 (2000).

[24] A. Albrecht and C. Skordis, Phys. Rev. Lett. **84**, 2076 (2000); E. J. Copeland, N. J. Nunes and F. Rosati, Phys. Rev. D **62**, 123503 (2000).

[25] B. A. Bassett, P. S. Corasaniti and M. Kunz, Astrophys. J. **617**, L1 (2004).

[26] A. G. Riess et al. [Supernova Search Team Collaboration], Astrophys. J. **607**, 665 (2004).

[27] D. N. Spergel *et al.* [WMAP Collaboration], Astrophys. J. Suppl. **148**, 175 (2003).

[28] R. J. Scherrer and A. A. Sen, Phys. Rev. D **77**, 083515 (2008).

[29] S. Dutta and R. J. Scherrer, Phys. Rev. D **78**, 123525

(2008).

[30] T. Chiba, Phys. Rev. D **79**, 083517 (2009).

[31] T. Chiba, S. Dutta and R. J. Scherrer, Phys. Rev. D **80**, 043517 (2009).

[32] T. Chiba, Phys. Rev. D **81**, 023515 (2010).

[33] P. S. Corasaniti, M. Kunz, D. Parkinson, E. J. Copeland and B. A. Bassett, Phys. Rev. D **70**, 083006 (2004).

[34] E. V. Linder and D. Huterer, Phys. Rev. D **72**, 043509 (2005).

[35] J. A. Frieman, C. T. Hill, A. Stebbins and I. Waga, Phys. Rev. Lett. **75**, 2077 (1995).

[36] R. R. Caldwell and E. V. Linder, Phys. Rev. Lett. **95**, 141301 (2005).

[37] W. Hu and I. Sawicki, Phys. Rev. D **76**, 064004 (2007); A. A. Starobinsky, JETP Lett. **86**, 157 (2007); S. A. Appleby and R. A. Battye, Phys. Lett. B **654**, 7 (2007); S. Tsujikawa, Phys. Rev. D **77**, 023507 (2008); H. Motohashi, A. A. Starobinsky and J. 'i. Yokoyama, Prog. Theor. Phys. **123**, 887 (2010).

[38] M. Baldi, Mon. Not. Roy. Astron. Soc. **420**, 430 (2012).

[39] V. Sahni, A. Shafieloo and A. A. Starobinsky, Phys. Rev. D **78**, 103502 (2008).

[40] E. E. O. Ishida, R. R. R. Reis, A. V. Toribio and I. Waga, Astropart. Phys. **28**, 547 (2008).

[41] A. C. C. Guimaraes and J. A. S. Lima, Class. Quant. Grav. **28**, 125026 (2011).

[42] R. Giostri, M. V. d. Santos, I. Waga, R. R. R. Reis, M. O. Calvao and B. L. Lago, arXiv:1203.3213 [astro-ph.CO].

[43] A. Shafieloo, V. Sahni and A. A. Starobinsky, Phys. Rev. D **80**, 101301 (2009).

[44] O. F. Piattella, D. Bertacca, M. Bruni and D. Pietrobon, JCAP **1001**, 014 (2010); D. Bertacca, M. Bruni, O. F. Piattella and D. Pietrobon, JCAP **1102**, 018 (2011).

[45] A. G. Riess *et al.*, Astrophys. J. **699**, 539 (2009).

[46] W. J. Percival *et al.*, Mon. Not. Roy. Astron. Soc. **401**, 2148 (2010).

[47] J. R. Bond, G. Efstathiou and M. Tegmark, Mon. Not. Roy. Astron. Soc. **291**, L33 (1997); Y. Wang and P. Mukherjee, Phys. Rev. D **76**, 103533 (2007).

[48] W. Hu and N. Sugiyama, Astrophys. J. **471**, 542 (1996).

[49] D. J. Eisenstein *et al.* [SDSS Collaboration], Astrophys. J. **633**, 560 (2005).

[50] D. J. Eisenstein and W. Hu, Astrophys. J. **496**, 605 (1998).

[51] C. Blake *et al.*, arXiv:1105.2862 [astro-ph.CO].

[52] F. Beutler *et al.*, Mon. Not. Roy. Astron. Soc. **416**, 3017 (2011).

[53] H. Akaike, IEEE Trans. Auto. Control, 19, 716 (1974); A. R. Liddle, Mon. Not. Roy. Astron. Soc. 351, L49 (2004).

[54] V. H. Cardenas and M. Rivera, Phys. Lett. B **710**, 251 (2012).